CHEMISTRY
A EUROPEAN JOURNAL

DOI: 10.1002/chem.200901364

Templated Synthesis of Copper(II) Azacyclam Complexes Using Urea as a Locking Fragment and Their Metal-Enhanced Binding Tendencies towards Anions

Massimo Boiocchi,[b] Luigi Fabbrizzi,*[a] Mauro Garolfi,[a] Maurizio Licchelli,*[a] Lorenzo Mosca,[a] and Cristina Zanini[a]

In memory of Professor Alan M. Sargeson

Abstract: Copper(II) azacyclam complexes $\mathbf{3}^{2+}$ and $\mathbf{4}^{2+}$ were obtained through a metal-templated procedure involving the pertinent open-chain tetramine, formaldehyde and a phenylurea derivative as a locking fragment. Both metal complexes can establish interactions with anions through the metal centre and the amide NH group. Equilibrium studies in DMSO by a spectrophotometric titration technique were carried out to assess the affinity of $\mathbf{3}^{2+}$ and $\mathbf{4}^{2+}$ towards anions. While the NH group of an amide model compound and the metal centre of the plain $Cu^{II}(azacyclam)^{2+}$ complex do not interact at all with anions, $\mathbf{3}^{2+}$ and $\mathbf{4}^{2+}$ establish strong interactions with oxo anions, profiting from a pronounced cooperative effect. In particular, 1) they form stable 1:1 and 1:2 complexes with $H_2PO_4^-$ ions in a stepwise mode with both hydrogen-bonding and metal–ligand interactions, and 2) in the presence of CH_3COO^-, they undergo deprotonation of the amido NH group and thus profit from axial coordination of the partially negatively charged carbonyl oxygen atom in a scorpionate binding mode.

Keywords: copper · macrocyclic ligands · receptors · scorpionates · template synthesis

Introduction

Metal-template syntheses lie at the heart of the chemistry of macrocycles[1,2] and provide effective tools for the development of supramolecular chemistry.[3] The prototype of tetraaza macrocycles, cyclam (**2**), could be obtained in high yield through Schiff base condensation of glyoxal with the open chain tetramine 3.2.3-tet (**1**), which is preoriented for cyclization by the Ni^{II} template.[4] The "reversible" C=N bond was hydrogenated, and made "irreversible", by $NaBH_4$. Cyclam can then be isolated by demetallation with cyanide in boiling basic solution and liquid–liquid extraction (see Scheme 1).[5]

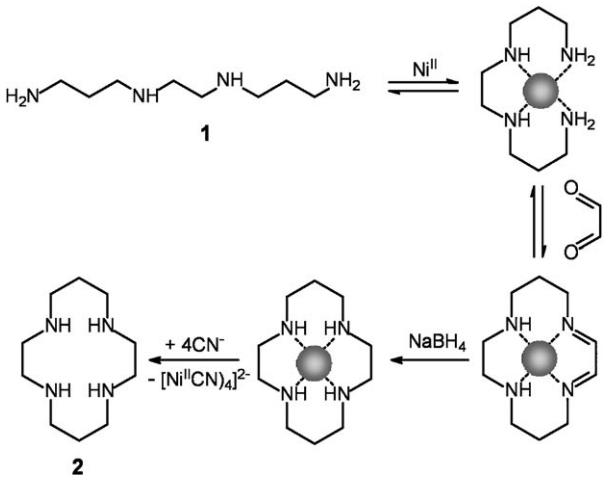

Scheme 1. Nickel(II)-templated synthesis of cyclam.[5]

Later, further convenient template syntheses of cyclam-like macrocycles and macrocyclic complexes were introduced, inspired by the classical Sargeson template syntheses of Co^{III} sepulchrate and sarcophagine (sar) complexes.[6,7] In the one-pot syntheses of these cage complexes, first six mol-

[a] Prof. L. Fabbrizzi, Dr. M. Garolfi, Prof. M. Licchelli, Dr. L. Mosca, Dr. C. Zanini
Dipartimento di Chimica Generale
Università di Pavia
via Taramelli 12, 27100 Pavia (Italy)
Fax: (+39) 0382-528544
E-mail: luigi.fabbrizzi@unipv.it

[b] Dr. M. Boiocchi
Centro Grandi Strumenti, Università di Pavia
via Bassi, 27100 Pavia (Italy)

ecules of formaldehyde undergo Schiff base condensation with the primary amino groups of $[Co^{III}(en)_3]^{3+}$ (en: 1,2-diaminoethane), and then two equivalents of a triprotic acid (NH_3[6] or CH_3NO_2),[7] in the presence of base, are deprotonated stepwise, and corresponding anions consecutively attack the imine bonds (synthesis of $[Co^{III}(diNOsar)]^{3+}$ is illustrated in Scheme 2). Astonishingly, 12 particles, organised by the cobalt centre, sequentially go to the right place in order to react and ultimately give the highly symmetric and aesthetically pleasing Co^{III} cage complex.[8]

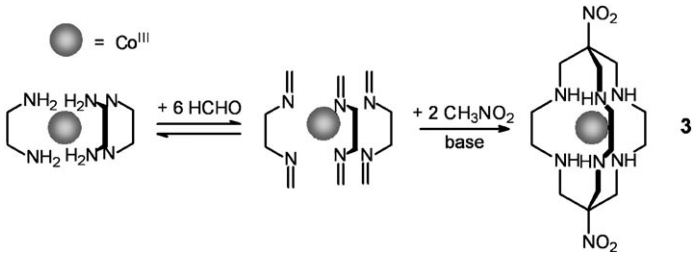

Scheme 2. Synthesis of $[Co^{III}(diNOsar)]^{3+}$ (diNOsar = dinitrosarcophagine).[7] CH_3NO_2 can be replaced by the other triprotic acid NH_3 to give the $[Co^{III}(sepulchrate)]^{3+}$ complex.[6]

The same strategy was then applied to the synthesis of cyclam-like macrocycles and macrocyclic complexes: in this case, a diprotic acid AH_2 is required to accomplish cyclization. For example, Sargeson et al. reported the reaction of two equivalents of nitroethane ($CH_3CH_2NO_2$) with $[Cu^{II}(ethylenediamine)_2]^{2+}$ in the presence of formaldehyde and base to give a dinitrocyclam complex (see Scheme 3, route a).[9]

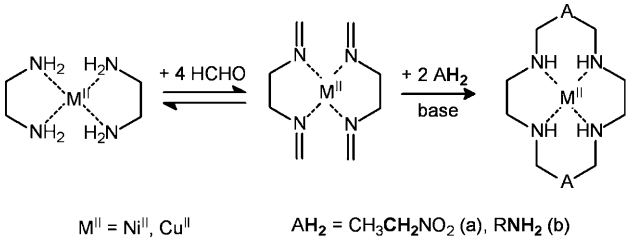

Scheme 3. Synthesis of cyclam-like macrocyclic complexes from bis-ethylenediamine complexes of Cu^{II} and Ni^{II} in the presence of formaldehyde and base by using a diprotic acid AH_2 as locking fragment.

Then, Suh and Kangly described the reaction of primary amines (CH_3NH_2, $C_2H_5NH_2$) with $[Ni^{II}(en)_2]^{2+}$ and $[Cu^{II}(en)_2]^{2+}$ (en = ethylenediamine) to give diazacyclam complexes (see Scheme 3, route b).[10] Cu^{II} or Ni^{II} ions could be used as a template in view of their propensity to form thermodynamically stable square-planar complexes with two en molecules. The nitroethane/formaldehyde approach has been used to cyclize linear tetramines of varying length to give Cu^{II} complexes with tetraaza macrocycles of ring size ranging from 13 to 16 members.[11] Also, primary anilines have been extensively used as locking fragments to give 14-membered azacyclam complexes. An interesting example is the reaction of melamine, which contains three aniline NH_2 fragments in the 1,3,5-positions of a phenyl ring, with three $[Cu^{II}(tetramine)]^{2+}$ complexes, in the presence of formaldehyde and base to give a trimetallic species of C_{3v} symmetry.[12,13]

We observed more recently that the NH_2 group of amides, both carboxyamides, $RC(O)NH_2$ and sulfonamides, $RS(O_2)NH_2$, works well as a locking fragment in the synthesis of Cu^{II}[14] and Ni^{II} azacyclam complexes (Scheme 4).[15]

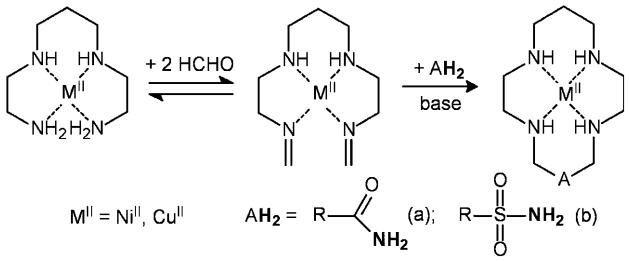

Scheme 4. Metal-templated synthesis of azacyclam complexes from complexes of Cu^{II} and Ni^{II} with a linear tetramine in the presence of formaldehyde and base by using a carboxyamide or a sulfonamide as locking fragment.

The good reactivity seems to be related to the relatively high acidity of amides. As carboxyamide or sulfonamide derivatives are in general easily attainable, this approach allows one to append to an azacyclam complex almost any desired functionality. Examples include a redox-active subunit (e.g., ferrocene)[16] and a fluorogenic fragment (e.g., naphthalene)[17] to give multifunctional molecular devices.[18,19]

We report here the synthesis of two novel Cu^{II} azacyclam complexes obtained through the reaction illustrated in Scheme 3, in which a phenylurea moiety was employed as a locking fragment (Scheme 5).

Metal azacyclam complexes $\mathbf{3}^{2+}$ and $\mathbf{4}^{2+}$ have an amide NH group which is polarised by the directly bound electron-withdrawing nitro- or cyanophenyl group. Secondary amido groups activated by electron-withdrawing substituents have been extensively used as hydrogen-bonding donors in the design of a variety of anion receptors.[20] We report here an investigation on how the proximate metal centre (which can

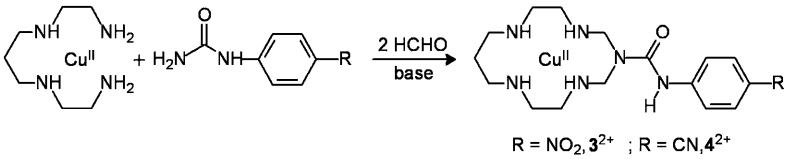

Scheme 5. Synthesis of copper(II) azacyclam complexes by using a phenylurea derivative as locking fragment.

interact with anions itself) modifies anion-recognition properties of the secondary amido group, and vice versa.

Equilibrium studies in polar DMSO medium have shown that the Cu^{II} azacylam subunit strongly increases the acidity of the amide NH group, inducing deprotonation in the presence of CH_3COO^- and favouring binding of the $H_2PO_4^-$ ion through simultaneous establishment of hydrogen-bonding and metal–ligand interactions. On the other hand, no interaction was observed with reference amides **5** and **6**. This indicates the special role played by the proximate metal azacyclam complex.

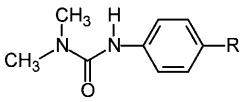

R = NO_2 **5**
R = CN **6**

A carboxyamide group was appended to the nitrogen atom of cyclen (1,4,7,10-tetraazacyclododecane) through reaction with aliphatic and aromatic isocyanates, and the interaction of the corresponding Cu^{II} and Zn^{II} complexes with DNA was investigated.[21]

Results and Discussion

Structure of azacyclam complexes: Figure 1 shows the molecular structures, determined by single crystal X-ray studies, of copper(II) azacyclam complexes $\mathbf{3}^{2+}$ and $\mathbf{4}^{2+}$, which were obtained as nitrate salts. Selected geometrical features around the Cu^{II} centres are reported in Table 1.

Both complexes exhibit an almost regular square-planar coordination geometry of the metal centre and the copper atoms deviate from the best plane of the four secondary amino groups by only 0.03(1) Å in $\mathbf{3}^{2+}$ and 0.10(1) Å in $\mathbf{4}^{2+}$. The two oxygen atoms of the nitrate counterions are located in the two axial positions of a rather elongated octahedron with Cu(1)–O(4) 2.41(1), Cu(1)–O(7) 2.55(1) Å for $\mathbf{3}^{2+}$ and Cu(1)–O(2) 2.41(1), Cu(1)–O(5) 2.64(1) Å for $\mathbf{4}^{2+}$. Such long interatomic distances suggest that the NO_3^- counterions may be involved in only very weak coordinative interactions.

Table 1. Selected bond lengths [Å] and bond angles [°] around the metal centre in $[\mathbf{3}](NO_3)_2$ and $[\mathbf{4}](NO_3)_2$ complex salts.

	$[\mathbf{3}](NO_3)_2$	$[\mathbf{4}](NO_3)_2$
Cu(1)–N(2)	2.021(5)	2.024(5)
Cu(1)–N(3)	2.003(5)	2.001(5)
Cu(1)–N(4)	1.990(5)	2.006(5)
Cu(1)–N(5)	2.009(5)	2.009(5)
N(2)-Cu(1)-N(3)	86.3(2)	85.7(2)
N(2)-Cu(1)-N(4)	178.3(2)	175.1(5)
N(2)-Cu(1)-N(5)	93.6(2)	94.6(2)
N(3)-Cu(1)-N(4)	94.0(2)	93.2(2)
N(3)-Cu(1)-N(5)	177.8(2)	173.3(2)
N(4)-Cu(1)-N(5)	86.2(2)	85.9(2)

The mean Cu–N distance is 2.01(1) Å for both azacyclam complexes $\mathbf{3}^{2+}$ and $\mathbf{4}^{2+}$. This value is only a bit shorter than the strain-free Cu–N distance of 2.03 Å reported for 14-membered tetraaza macrocycles.[22] The tertiary nitrogen atom of each azacyclam ring is not involved in coordination and plays a mere architectural role; it shows a nearly trigonal-planar geometry, sp^2 hybridization and pronounced involvement of the lone pair in the amide bond.

In both complexes, the cyclam-like ring is present as the *R*,*S*,*S*,*R* diastereoisomer (also denoted *trans*-III form),[23] the most stable and most frequently observed configurational isomer of metal complexes with the unsubstituted cyclam ligand.[24] Similar bond lengths, bond angles and configuration have been observed in previously investigated carboxyamide-functionalised Cu^{II} azacyclam complexes.[25] The phenylamide group points outward from the metal centre, leaving open room for coordination of further ligands to Cu^{II}.

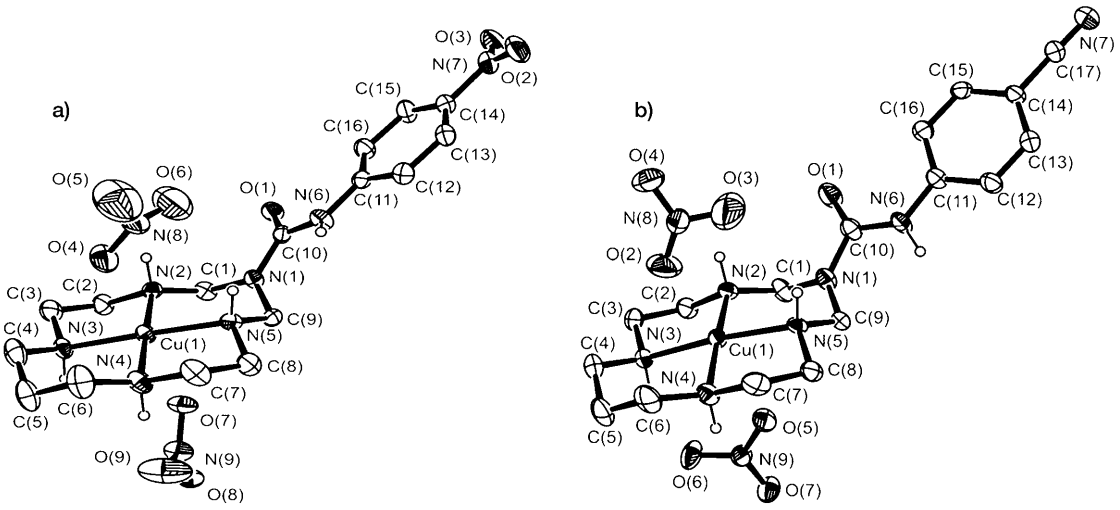

Figure 1. ORTEPs of copper(II) azacyclam complex salts $[\mathbf{3}](NO_3)_2$ (a), and $[\mathbf{4}](NO_3)_2$ (b). Thermal ellipsoids are drawn at 30% probability; only H atoms bonded to N_{amine} atoms are shown.

Anion binding: equilibrium studies with model amides: Anion interactions with neutral receptors like amides are typically investigated in aprotic media ($CHCl_3$, MeCN, DMSO) to avoid competition of the solvent in donating H-bonds to the anion. Moreover, the stability of the receptor–anion association complexes decreases along the series $CHCl_3 > MeCN > DMSO$, which reflects increasing solvent polarity and higher energy spent in desolvating the anion.[26] The present study was carried out in DMSO, due to the very poor solubility of ionic complexes $\mathbf{3}^{2+}$ and $\mathbf{4}^{2+}$ in less polar solvents.

Binding tendencies of the amide NH group towards anions were investigated by carrying out spectrophotometric titration experiments. In a typical experiment, a 5×10^{-5} M solution of the receptor was titrated with a 5×10^{-3} M solution of the tetrabutylammonium salt of the envisaged anion. On light absorption, metal-containing phenylurea derivatives $\mathbf{3}^{2+}$ and $\mathbf{4}^{2+}$, as well as reference metal-free amides **5** and **6**, give rise to a charge-transfer transition, basically from the nitrogen atom of the NH group to the electron-withdrawing substituent (NO_2 or CN), along the phenyl ring, which results in a rather intense absorption band in the UV region. The optical transition generates a partial negative charge on the substituent and a partial positive charge on the amide nitrogen atom. Thus, interaction of a negatively charged ion at the NH group is expected to stabilise the excited state and thus reduce the energy of the transition. As a consequence, on interaction with the anion, a red shift of the absorption band should be observed. The stronger the anion–receptor interaction, the more pronounced the red shift.

To assess the hydrogen-bonding donor tendencies of the amide group in the absence of any cooperative effect of the proximate metal centre, preliminary titration experiments were carried out for reference amides **5** and **6** in DMSO solution. However, even on addition of a large excess of the more basic anions (CH_3COO^- and $H_2PO_4^-$) no significant spectral modification were observed. In particular, no shift of the charge-transfer transition bands centred at 350 (**5**, $\varepsilon=13400$) and at 280 nm (**6**, $\varepsilon=24400\ cm^{-1}M^{-1}$) was detected. To verify binding tendencies towards anions of amides **5** and **6**, the same titration experiments were carried out also in the less polar solvent MeCN. However, also in this case, no spectral changes were observed. This indicates that receptor–anion association constants are smaller than 100 and demonstrates the poor donating tendencies of a single NH group towards anions. Indeed, the numerous investigated amide-based anion receptors contain several NH groups, strategically placed inside a cavity.[27]

Interaction of Cu^{II} azacyclam complexes $\mathbf{3}^{2+}$ and $\mathbf{4}^{2+}$ with CH_3COO^-: metal-assisted amide deprotonation: Figure 2a shows spectra taken over the course of titration of a 5×10^{-5} M solution of Cu^{II} azacyclam complex $\mathbf{3}^{2+}$, $[Cu^{II}(LH)]^{2+}$, in DMSO with $[Bu_4N]CH_3COO$. The receptor shows a rather intense band centred at 330 nm, responsible for the pale yellow colour.

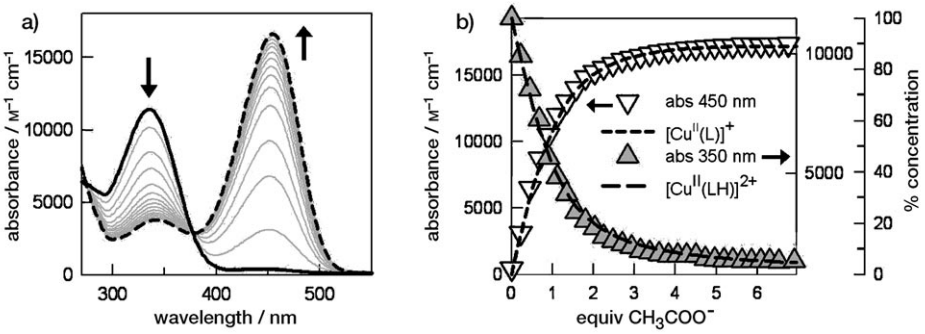

Figure 2. a) Spectra taken over the course of the titration of a 5×10^{-5} M solution of Cu^{II} azacyclam complex $\mathbf{3}^{2+}$, $[Cu^{II}(LH)]^{2+}$, in DMSO with a 4.5×10^{-3} M DMSO solution of $[Bu_4N]CH_3COO$. b) Dashed lines: concentration of the undeprotonated $[Cu^{II}(LH)]^{2+}$ and deprotonated $[Cu^{II}(L)]^{+}$ species (off right vertical axis); symbols: absorbance of the bands centred at 350 nm for $[Cu^{II}(LH)]^{2+}$ (right vertical axis) and 450 nm for $[Cu^{II}(L)]^{+}$ (left vertical axis).

On addition of acetate, the solution progressively takes on a bright yellow colour, while the intensity of the band at 330 nm decreases and a new band forms and develops at 450 nm. Such large red shifts of charge-transfer bands of amide (and urea) receptors (100 nm in the present case) and drastic colour changes are typically associated with deprotonation of the NH group.[28–31] Thus, the occurrence of an acid–base neutralisation equilibrium is suggested [Eq. (1)]

$$[Cu^{II}(LH)]^{2+} + CH_3COO^- \rightleftharpoons [Cu^{II}(L)]^{+} + CH_3COOH \qquad (1)$$

Best fitting of spectrophotometric titration data with a non-linear least-squares procedure[32] over the interval 250–550 nm was obtained by assuming a 1:1 equilibrium with $\log K = 4.807 \pm 0.03$. Figure 2b shows the percentage concentrations of undeprotonated $[Cu^{II}(LH)]^{2+}$ and deprotonated $[Cu^{II}(L)]^{+}$, calculated on the basis of the $\log K$ value. Occurrence of equilibrium (1) is confirmed by the fact that 1) the absorbance of the $\mathbf{3}^{2+}$ receptor (e.g., taken at 350 nm) superimposes well on the concentration profile of $[Cu^{II}(LH)]^{2+}$ and 2) the absorbance of the band at 450 nm superimposes well on the concentration profile of $[Cu^{II}(L)]^{+}$. Acetate-induced deprotonation of an NH group in DMSO was previously observed for thiourea derivatives bearing strongly electron withdrawing substituents.[33] Thiourea is a distinctly stronger acid than urea in DMSO (pK_a values: 21.1 and 26.95, respectively).[34] Moreover, in the mentioned case,[33] two stepwise equilibria occurred: first, the formation of a genuine thiourea/acetate H-bonded complex, then deprotonation of the NH group with simultaneous formation of the $[CH_3COOH\cdots CH_3COO]^-$ H-bonded self-complex. Quite

surprisingly, in the present case, acetate-induced deprotonation of the NH group 1) takes place with the less acidic urea subunit, and 2) does not involve formation of the $[CH_3COOH\cdots CH_3COO]^-$ complex, but occurs directly on addition of only 1 equiv of acetate. This evidence points towards a significant cooperative effect exerted by the Cu^{II}–azacyclam subunit and, in particular, by the Cu^{II} centre. However, no information on the state of the Cu^{II} centre over the course of the titration can be inferred from absorption spectra, because the intense charge-transfer band of the deprotonated species covers the wavelength interval in which d–d bands of Cu^{II}(azacyclam)$^{2+}$ complexes are typically observed.

The situation may be more convenient in the case of the Cu^{II} derivative $\mathbf{4}^{2+}$, in which a cyanophenyl substituent is present. In fact, the charge-transfer transition of the cyanophenylamide unit takes place below 300 nm, and the band pertinent to the deprotonated form, if any, should not interfere with d–d transitions. Figure 3 shows the family of spectra obtained during the titration of a 5×10^{-5} M solution of Cu^{II} azacyclam complex $\mathbf{4}^{2+}$, $[Cu^{II}(LH)]^{2+}$, in DMSO with $[Bu_4N]CH_3COO$.

The spectrophotometric response is analogous to that observed for $\mathbf{3}^{2+}$. In the present case, the functionalised Cu^{II} azacyclam complex, before acetate addition, shows an intense absorption band, centred at 270 nm, which originates from the optical transition from the *N,N′*-dialkylurea subunit to the cyano group. This band is centred at a higher energy than in the nitro derivative, due to the lower intensity of the transition dipole. Acetate addition makes the band at 270 nm decrease, while a new intense band forms and develops at 330 nm. Again, this strongly red-shifted band is ascribed to the deprotonated species $[Cu^{II}(L)]^{2+}$, which forms according to an acid–base equilibrium of type (1). The $\log K$ value for proton transfer from the amide NH group to CH_3COO^- is 4.35 ± 0.03, that is, 0.5 units lower than for $\mathbf{3}^{2+}$, a difference which may reflect the stronger polarizing effect exerted by the nitro group. Conveniently, the band of the deprotonated form of $\mathbf{4}^{2+}$, $[Cu^{II}(L)]^{+}$, appears at relatively high energy and leaves the visible region, where d–d transitions take place uncovered.

Figure 4a shows d–d spectra taken during the titration of a 1.02×10^{-3} M solution of $\mathbf{4}^{2+}$ in DMSO with $[Bu_4N]CH_3COO$. The band centred at 510 nm (short dashes in Figure 4a) is that typically observed for a Cu^{II}(azacyclam)$^{2+}$ complex with square-planar coordination geometry (as shown, for instance, by the crystal and molecular structure in Figure 1a). On CH_3COO^- addition, the band is shifted to higher wavelength and increases in intensity. Such behaviour is indicative of a change from fourfold coordination with square-planar geometry to fivefold coordination, probably with square-pyramidal geometry. In particular, the broad band at 510 nm must be considered as an envelope of three bands resulting from $xz,yz\rightarrow x^2-y^2$, $z^2\rightarrow x^2-y^2$ and $xy\rightarrow x^2-y^2$ transitions the square-planar complex.[35] Approach of a fifth donor atom along the z axis raises the energy of the levels with a z component, and this results in a decrease in the energy of pertinent transitions of and ultimately causes a shift of the envelope to higher wavelengths. Moreover, on interaction of a fifth donor atom, the azacyclam complex loses its centre of symmetry, a circumstance which renders d–d

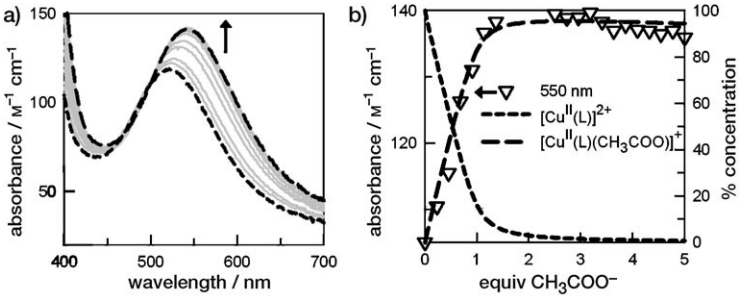

Figure 4. a) Spectra taken over the course of the titration of a 1.02×10^{-3} M solution of the Cu^{II} azacyclam complex $\mathbf{4}^{2+}$, $[Cu^{II}(LH)]^{2+}$, in DMSO with a 0.102 M DMSO solution of $[Bu_4N]CH_3COO$. b) Dashed lines: concentration of undeprotonated $[Cu^{II}(LH)]^{2+}$ and deprotonated $[Cu^{II}(L)]^{+}$ species (right vertical axis); symbols: absorbance of the band centred at 550 nm for $[Cu^{II}(L)]^{+}$ (left vertical axis).

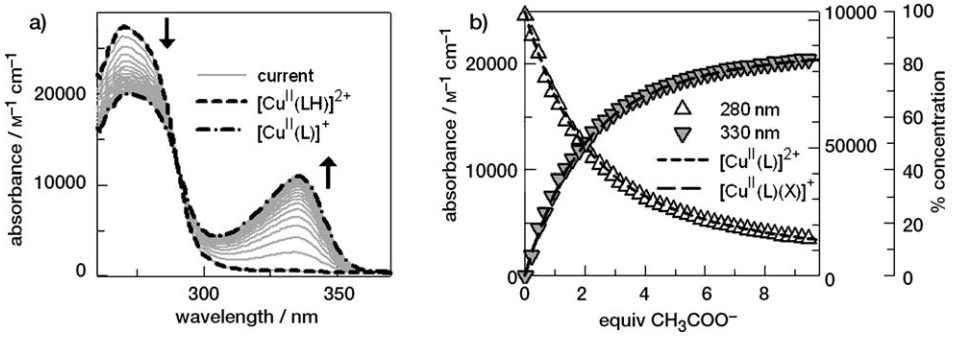

Figure 3. a) Spectra taken over the course of the titration of a 5×10^{-5} M solution of the Cu^{II} azacyclam complex $\mathbf{4}^{2+}$, $[Cu^{II}(LH)]^{2+}$ in DMSO with a 4.5×10^{-3} M DMSO solution of $[Bu_4N]CH_3COO$. b) Dashed lines: concentration of the undeprotonated $[Cu^{II}(LH)]^{2+}$ and deprotonated $[Cu^{II}(L)]^{+}$ species (off right vertical axis); b) symbols: absorbance of the bands centred at 280 nm for $[Cu^{II}(LH)]^{2+}$ (right vertical axis) and at 330 nm for $[Cu^{II}(L)]^{+}$ (left vertical axis).

transitions "less" forbidden and increases the absorbance.[36] On this basis, we suggest that the fifth donor atom is the carbonyl oxygen atom of the urea subunit, which, on deprotonation of the NH group, takes on a partial negative charge. The process is tentatively illustrated in Scheme 6.

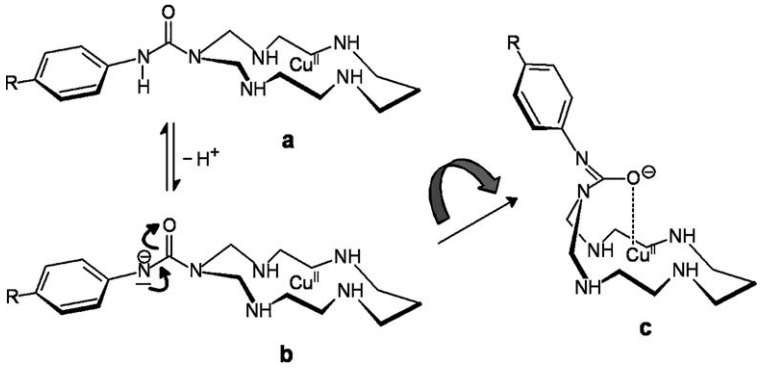

Scheme 6. Metal-induced deprotonation of the secondary amide group. The deprotonation process is made feasible by coordination of the partially negatively charged carbonyl oxygen atom to the Cu^{II} centre.

Macrocycles with a movable pendant arm whose coordinating tendencies can be switched on/off by an external input (e.g., a change of pH) are called scorpionands.[37] One of the first examples was the the Ni^{II} complex of *N*-aminoethylcyclam.[38] At pH < 3, the amine group is protonated and the pendant arm stays far away from the metal centre (Scheme 7a); at pH > 3, the amino group is no longer protonated and binds to the metal centre from the top, like the tail of a scorpion (Scheme 7b).

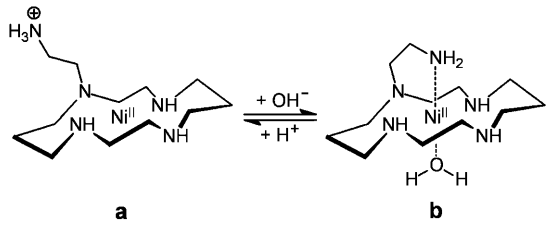

Scheme 7. Metal scorpionate equilibrium. Deprotonation of the ethylammonium side chain induces axial binding of the primary amine group, with a change of the coordination geometry from square-planar (a) to octahedral (b).[37]

Systems $\mathbf{3}^{2+}$ and $\mathbf{4}^{2+}$ are new examples of scorpionate complexes, the uncoordinated (**a** in Scheme 6) or coordinated (**c**) state of which is changed through an auxiliary acid–base reaction ($CH_3COO^- + H^+ \rightleftarrows CH_3COOH$). Thus, the acidic behaviour of the amide NH group, which is not observed at all in the model compounds **5** and **6**, seems to be solely determined by coordination to the proximate metal centre of the carbonyl oxygen atom, which, on NH deprotonation, takes on a partial negative charge. On addition of acid (e.g., CF_3SO_3H), the deprotonated amide group takes on one proton, the carbonyl oxygen atom loses the partial negative charge and the system is reset to state **a** (as indicated by the full restoration of the charge-transfer bands at 330 ($\mathbf{3}^{2+}$) and at 270 nm ($\mathbf{4}^{2+}$). Coordination of the C=O group in a scorpionate mode prior to acetate addition can be ruled out for two main reasons: 1) the structures of the complex salts $[\mathbf{3}](NO_3)_2$ and $[\mathbf{4}](NO_3)_2$ shown in Figure 1 indicate that the phenylamide pendant arm points outwards from the metal centre; 2) the d–d band of $\mathbf{4}^{2+}$ appears at the same wavelength as those of Cu^{II} complexes with cyclam and azacyclam derivatives not bearing a carboxyamide group, while axial perturbation would cause a definite red shift.

Interaction of the Cu^{II}-azacyclam complexes 3 and 4 with $H_2PO_4^-$: metal-assisted formation of H-bonded complexes: The $H_2PO_4^-$ ion is distinctly less basic than CH_3COO^- (pK_A values in water: 1.97[39] and 4.76,[40] respectively) and does not induce deprotonation of the amide NH group of Cu^{II} azacyclam complexes $\mathbf{3}^{2+}$ and $\mathbf{4}^{2+}$; in fact, it gives genuine association complexes, held together by H-bonds and metal–ligand interactions, as shown by unambiguous spectrophotometric evidence.

Figure 5a shows spectra taken over the course of the titration of a dilute solution (5×10^{-5} M) of $\mathbf{4}^{2+}$, $[Cu^{II}(LH)]^{2+}$, with $[Bu_4N]H_2PO_4$. Addition of the anion induces a moderate red shift of the charge-transfer band centred at 270 nm, the maximum of which, after addition of an excess of phosphate, is red-shifted by about 10 nm. Such behaviour is typically observed in phenylurea derivatives following H-bonding interaction of anions at the NH group.[28–31] Best fitting of titration data was obtained by assuming the presence of two complex species at equilibrium, one containing one phosphate anion, and the other two phosphate anions, formed according to two stepwise processes [Eqs. (2) and (3)].

$$[Cu^{II}(LH)]^{2+} + H_2PO_4^- \rightleftharpoons [Cu^{II}(LH)(H_2PO_4)]^+ \quad (2)$$

$$[Cu^{II}(LH)(H_2PO_4)]^+ + H_2PO_4^- \rightleftharpoons [Cu^{II}(LH)(H_2PO_4)_2] \quad (3)$$

The equilibrium constants for the two stepwise equilibria are $\log K_1 = 4.27 \pm 0.01$ and $\log K_2 = 3.66 \pm 0.04$ for Equations (2) and (3), respectively. Figure 5b shows how the concentration of the three species at equilibrium, $[Cu^{II}(LH)]^{2+}$, $[Cu^{II}(LH)(H_2PO_4)]^+$ and $[Cu^{II}(LH)(H_2PO_4)_2]$, vary over the course of titration with phosphate. The decreasing absorbance of the band centred at 270 nm superimposes well on the decreasing profile of the concentration of the uncomplexed receptor $[Cu^{II}(LH)]^{2+}$. On the other hand, the absorbance of the red-shifted band, centred at 280 nm, maxi-

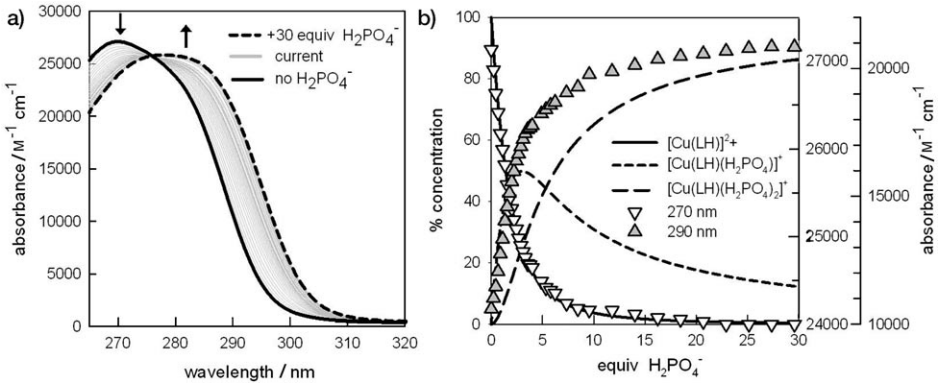

Figure 5. a) Spectra taken over the course of the titration of a 5×10^{-5} M solution of the Cu^{II} azacyclam complex $\mathbf{4}^{2+}$, $[Cu^{II}(LH)]^{2+}$, in DMSO with $[Bu_4N]H_2PO_4$. b) Long-dashed line: concentration of the receptor $[Cu^{II}(LH)]^{2+}$; short-dashed line: concentration of 1:1 complex $[Cu^{II}(L)(H_2PO_4)]^+$; dash-dotted line: concentration of 1:2 complex $[Cu^{II}(LH)(H_2PO_4)_2]$ (off right vertical axis); symbols: ▲, absorbance at 320 nm, monitoring the decreasing concentration of the receptor $[Cu^{II}(LH)]^{2+}$ (right vertical axis); ▼: absorbance at 370 nm, monitoring the increasing concentration of both $[Cu^{II}(LH)(H_2PO_4)]^+$ and $[Cu^{II}(LH)(H_2PO_4)_2]$ (left vertical axis).

mum intensity of which is achieved after addition of about 20 equiv of $H_2PO_4^-$, seems to be associated with formation of both 1:1 and 1:2 receptor:anion complexes, as it develops on initial anion addition, when $[Cu^{II}(LH)(H_2PO_4)]^+$ forms, and keeps increasing as the concentration of $[Cu^{II}(LH)(H_2PO_4)]^+$ decreases and the concentration of $[Cu^{II}(LH)(H_2PO_4)_2]$ rises. However, prior to putting forward any hypothesis on the nature and geometry of the 1:1 and 1:2 association complexes, it is useful to assess whether the metal centre is involved in the interaction with the anion. Thus, the same titration experiment was carried out on a more concentrated solution (1.40×10^{-3} M), in order to detect changes in the d–d spectrum of the Cu^{II}–azacyclam subunit of $\mathbf{4}^{2+}$.

Figure 6a shows spectra recorded during the titration with phosphate. It is observed that on anion addition the d–d band pertinent to the $[Cu^{II}(LH)]^{2+}$ receptor undergoes a definite red shift and a significant increase in intensity. Such spectral modifications point towards establishment of coordinative $Cu^{II}/H_2PO_4^-$ interactions. The titration profile in Figure 6b (absorbance at 550 nm vs. equiv of phosphate) reaches saturation on addition of 2 equiv of the anion. This unambiguously indicates that both the first and the second $H_2PO_4^-$ anion interact with the Cu^{II} centre of the $\mathbf{4}^{2+}$ receptor. This may be surprising, if one considers the behaviour of reference azacyclam complex **7**.

On addition of an excess of $H_2PO_4^-$ to a 10^{-3} M of **7** in DMSO, no modifications were observed in the d–d band. This indicates that the phosphate ion has a poor affinity towards

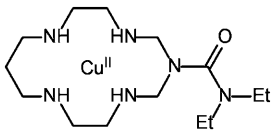

7

the Cu^{II} centre of the azacyclam complex in a DMSO solution and, in any case, it is not able to displace solvent molecules, which are present in an overwhelming amount, from the apical positions of the elongated coordination octahedron. This suggests that, in complex $\mathbf{4}^{2+}$, phosphate binding to the metal centre must be driven by an additional interaction: hydrogen bonding, as tentatively illustrated in Scheme 8.

We hypothesise that in the first step one of the two oxygen atoms of the $H_2PO_4^-$ ion bearing a partial negative charge binds to the Cu^{II} centre, while the other partially negatively charged oxygen atom receives an H-bond from the amide NH group. In the second step, an $H_2PO_4^-$ ion binds to the Cu^{II} ion through the oxygen atom that formally bears a full negative charge, while one of its OH groups donates an H-bond to the carbonyl oxygen atom of the pendant phenylurea subunit. According to Scheme 8, the first step profits firstly from coordinative interaction of the Cu^{II} ion with an oxygen atom with a formal charge of $-1/2$ and secondly from an H-bonding interaction involving a nitrogen atom and

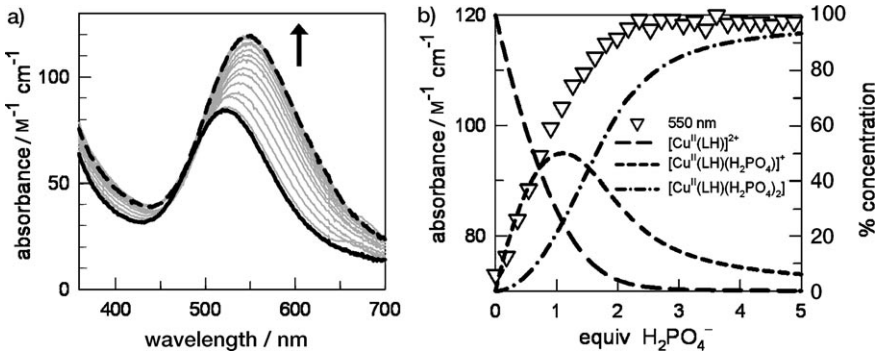

Figure 6. a) Spectra taken over the course of the titration of a 1.40×10^{-3} M solution of Cu^{II} azacyclam complex $\mathbf{4}^{2+}$, $[Cu^{II}(LH)]^{2+}$, in DMSO with a 0.101 M DMSO solution of $[Bu_4N]H_2PO_4$. b) Dashed lines: concentration of the $[Cu^{II}(LH)]^{2+}$ receptor and of the anion association complexes $[Cu^{II}(L)(H_2PO_4)]^+$ and $[Cu^{II}(L)(H_2PO_4)_2]$ (right vertical axis); symbols: absorbance of the d–d band centred at 550 nm for $[Cu^{II}(LH)]^{2+}$ (right vertical axis) and at 550 nm for $[Cu^{II}(L)]^+$ (left vertical axis).

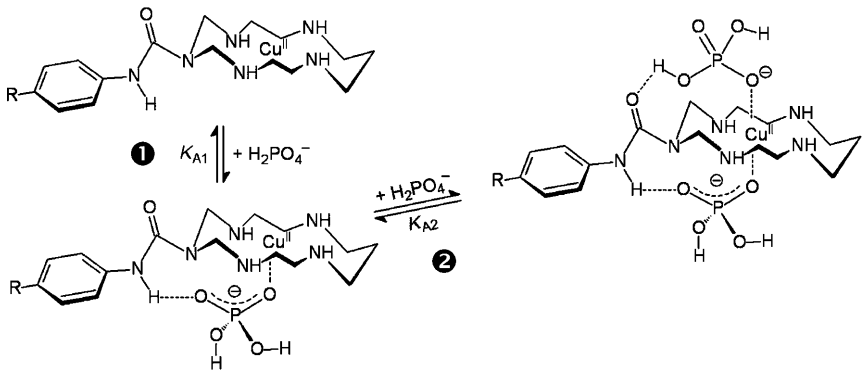

Scheme 8. Hypothesised two-step binding of $H_2PO_4^-$ to a $Cu^{II}(azacyclam)^{2+}$ complex acting as a ditopic anion receptor (R = NO_2, $\mathbf{3}^{2+}$; CN, $\mathbf{4}^{2+}$).

an oxygen atom with a formal charge of $-1/2$. Then, the second step profits 1) from the metal–ligand interaction of Cu^{II} with an oxygen atom with a formally integer negative charge (more exothermic effect) and 2) from H-bonding involving neutral oxygen atoms (less exothermic). The two overall energy contributions should be of comparable magnitude and, therefore, the sequence of steps illustrated in Scheme 7 could be reasonably inverted.

In the case of the nitro derivative $\mathbf{3}^{2+}$, $\log K_1$ (3.90 ± 0.04) and $\log K_2$ (4.01 ± 0.06) are coincident (within standard deviations). This may be surprising, because, other terms being the same, $\log K_1$ should be 0.6 units larger than $\log K_2$, due to the statistical effect ($=\log 4$). However, other factors can contribute, such as the different degrees of freedom of the receptor before and after interaction with the first phosphate ion: in particular, the rigidified $[Cu^{II}(LH)]^{2+}$ complex will experience a lower entropy loss when binding the second phosphate anion. Moreover, slightly different conformational arrangement of receptors $\mathbf{3}^{2+}$ and $\mathbf{4}^{2+}$, as evidenced by X-ray structure determination, can account for the different patterns of $\log K_1$ and $\log K_2$ values. In any case, $\log \beta_2$ values ($=\log K_1 + \log K_2$) are the same for both $\mathbf{3}^{2+}$ and $\mathbf{4}^{2+}$ receptors (7.9 log units), which indicates a substantial balance of energy contributions in the interaction of each amide-functionalised azacyclam complex with two phosphate anions.

In polar non-aqueous solvents, the $H_2PO_4^-$ ion may form H-bonded dimers, as illustrated by formula **8** in Figure 7, which also shows the structure of the dimer observed in the crystal structure of the isolated receptor/anion complex, in which the receptor is a bis-urea derivative.[41] Thus, one cannot exclude that the $[Cu^{II}(LH)(H_2PO_4)]^+$ complex undergoes a dimerisation process [Eq. (4)].

$$2\,[Cu^{II}(LH)(H_2PO_4)]^+ \rightleftharpoons [\{Cu^{II}(LH)(H_2PO_4)\}_2]^{2+} \qquad (4)$$

In the dimeric complex $[\{Cu^{II}(LH)(H_2PO_4)\}_2]^{2+}$, the diphosphate core should bridge two $[Cu^{II}(LH)]^{2+}$ complexes, and bonding at the right and left sides of formula **8** should involve a combination of H-bonding and metal–ligand interactions, as hypothesised for the monomeric complex. Spectral features cannot help to discriminate the $[Cu^{II}(LH)(H_2PO_4)]^+$ and $[\{Cu^{II}(LH)(H_2PO_4)\}_2]^{2+}$ complexes, as the Cu^{II} centre in both complexes would experience interactions with the same set of donor atoms. However, formation of a stable dimeric species, fully saturated and not inclined to react with a further phosphate ion, would imply that spectral modifications stop after the addition of one equivalent of $H_2PO_4^{2-}$. The fact that the titration profile (see triangles in Figure 6b) reaches a plateau only on addition of two equivalents of anion strongly supports the occurrence of two stepwise equilibria, as described by Equations (2) and (3), according to the mechanism illustrated in Scheme 8.

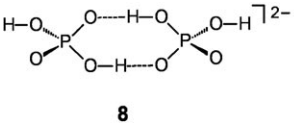

8

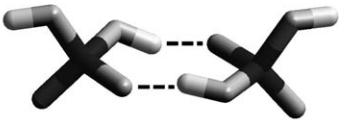

Figure 7. The H-bonded dimeric complex $[H_2PO_4 \cdots H_2PO_4]^{2-}$ (**8**), which may form in polar non-aqueous media, for example, DMSO; on the right side, the structure of the dimer, as observed in the crystal structure of the complex with 1,1-(4-nitrophenyl)-3-{2-[3-(4- nitrophenyl)ureido]cyclohexyl}urea is shown.[41] Dashed lines indicate H-bonding interactions (O–H···O). Structure redrawn from data deposited at the Cambridge Crystallographic Data Centre: CCDC-268368.

In conclusion, the phosphate ion, in DMSO solution, does not show any affinity towards the NH groups of model amide derivatives **5** and **6** or towards the Cu^{II} centre in the amide-NH-free azacyclam complex **7**. However, it forms stable 1:1 and 2:1 association complexes with receptors $\mathbf{3}^{2+}$ and $\mathbf{4}^{2+}$, thanks to establishing two-point interactions of H-bonding and metal–ligand nature with the receptor and a significant cooperative effect.

Interestingly, only CH_3COO^- and $H_2PO_4^-$ are able to interact with receptors $\mathbf{3}^{2+}$ and $\mathbf{4}^{2+}$. Less basic oxoanions, for example, HSO_4^- and NO_3^-, even if added in a large excess, do not modify the UV and visible absorption spectra of both amide functionalised azacyclam complexes. No effect was observed also on addition of Cl^-, Br^- and I^-, a behaviour which reflects their inability to act as a bridging ligand in receptors $\mathbf{3}^{2+}$ and $\mathbf{4}^{2+}$.

Conclusions

This work has demonstrated the versatility of metallo-azacyclam-based systems as anion receptors. In particular, the proximate metal centre dramatically enhances the intrinsically poor H-bond donor tendencies of a single secondary amide group through two distinctive cooperative effects:

1) in the presence of an ion that is not too basic, such as $H_2PO_4^-$, the Cu^{II}–azacyclam receptor provides multiple binding sites for formation of 1:1 and 1:2 association complexes, whose high stability in solution seems to be related to a favourable geometrical complementarity between receptor and anion(s); 2) in the case of the more basic CH_3COO^- ion, the receptor offers an intramolecular binding mechanism for coordination of the carbonyl oxygen atom, which favours deprotonation of the amide group, a process never observed in the presence of acetate. Moreover, coordination of the tetramine macrocycle provides two unique and functional features: 1) open space for coordination of further ligands, including anions, in the apical positions of an elongated octahedron; 2) high kinetic resistance to demetallation, even in the presence of a large excess of anions.

Experimental Section

General procedures and materials: All reagents for syntheses were purchased from Aldrich/Fluka and used without further purification. 1,3-Bis(2-aminoethylamino)propane was synthesised according to a reported procedure.[42] All reactions were performed under a dinitrogen atmosphere. UV/Vis spectra were recorded on a Varian CARY 50 or CARY 100 spectrophotometer with quartz cuvettes of the appropriate path length (0.1 or 1 cm). The concentration of the chromophore and the optical path were adjusted to obtain spectra with $AU \leq 1$. In titrations with anions, spectra of samples were recorded after addition of aliquots of the tetraalkylammonium salt of the envisaged anion under an inert atmosphere. IR spectra were recorded on a Perkin-Elmer Spectrum BX FTIR instrument; samples were finely ground and dispersed in Nujol, NaCl windows were used. Mass spectra were acquired on a Thermo-Finnigan ion-trap LCQ Advantage Max instrument equipped with an ESI source.

Synthesis of phenylureas 8 and 9: The appropriate 4-substituted phenylisocyanate was dissolved in diethyl ether (30 mL) with vigorous stirring. Gaseous ammonia was bubbled through the ethereal solution until complete precipitation occurred. Vacuum filtration, followed by washing with portions of cold diethyl ether, afforded the desired product in a high yield.

4-Nitrophenylurea (8): 4-Nitrophenylisocyanate (0.57 g, 3.47 mmol); 4-nitrophenylurea (0.56 g, 3.09 mmol, 89%); pale yellow powder. ESI-MS: (−): *m/z* (%): 180.2 $[M-H]^-$ (54), 226.1 $[M+HCOO]^-$ (100); IR: (Nujol): $\tilde{\nu}=3500$, 3317, 3279, 3154, 3093 (NH stretch); 1690 (CO stretch); 1560, 1322 cm^{-1} (NO_2 sym. and asym. stretch).

4-Cyanophenylurea (9): 4-Cyanophenylisocyanate (1 g, 6.94 mmol); 4-cyanophenylurea (1.08 g, 6.70 mmol, 96.5%); white powder; ESI-MS (−): *m/z* : 383.6 $[2M+NO_3]^-$ (100). IR: (Nujol): $\tilde{\nu}=3483$, 3378 (NH stretch), 1676 (CO stretch); 2219 cm^{-1} (CN stretch).

Synthesis of *N*′,*N*′-dimethyl-*N*-phenylureas 5 and 6: The corresponding 4-substituted phenyl isocyanate was dissolved in diethyl ether (30 mL) with vigorous stirring. Gaseous dimethylamine (generated by warming 5 mL of 40% aqueous dimethylamine) was bubbled through the organic phase until complete precipitation occurred. The precipitate was collected by vacuum filtration and washed with portions of cold diethyl ether, to afford the desired product in a high yield.

***N*′,*N*′-Dimethyl-*N*-(4-nitrophenyl)urea (5)**: 4-Nitrophenylisocyanate (0.31 g, 1.89 mmol); *N*′,*N*′-dimethyl-*N*-(4-nitrophenyl)urea (0.35 g, 1.69 mmol, 89.4%). ESI-MS (−): *m/z* (%): 208.4 $[M-H]^-$ (25), 244.2 $[M+Cl]^-$ (44), 254.0 $[M+HCOO]^-$ (100), 452.8 $[2M+Cl]^-$ (75), 462.7-$[2M+HCOO]^-$ (33); IR (Nujol): $\tilde{\nu}=3340$ (NH stretch), 1652 (CO stretch), 1538, 1325 cm^{-1} (NO_2 sym. and asym. stretch).

***N*′,*N*′-Dimethyl-*N*-(4-cyanophenyl)urea (6)**: 4-Cyanophenylisocyanate (0.29 g, 2.01 mmol); *N*′,*N*′-dimethyl-*N*-(4-cyanophenyl)urea (0.25 g, 1.32 mmol, 65.7%). ESI-MS (−): *m/z*: 302.3 $[M+CF_3COO]^-$ (89), 413.1 $[2M+Cl]^-$ (100), 439.9 $[2M+NO_3]^-$ (63), 490.6 $[2M+CF_3COO]^-$ (96); IR (Nujol): $\tilde{\nu}=3297$ (NH stretch), 1653 (CO stretch); 2218 cm^{-1} (CN stretch).

Copper(II) azacyclam complex [3](NO$_3$)$_2$: $Cu(NO_3)_2 \cdot 3H_2O$ (0.63 g, 2.6 mmol) dissolved in ethanol (10 mL), 1,3-bis(2′-aminoethylamino)propane (0.40 g, 2.5 mmol) in EtOH (15 mL) and 4-nitrophenylurea (**8**, 0.45 g, 2.5 mmol) in EtOH (30 mL) were placed in a screw-capped glass vial. To this solution triethylamine (0.75 mL, 5.4 mmol) and aqueous formaldehyde (36.5%, 2 mL, 26.5 mmol) were subsequently added . The reaction container was kept for three days in a oven adjusted to 75 °C. A deep violet solid formed at the bottom of the container, and the solvent was decanted. The solid was washed with small portions of ethanol and collected by filtration under vacuum to yield 0.36 g of the crystalline complex salt (0.65 mmol, 27.4%). ESI-MS (+): *m/z* (%): 490.1 $[M+NO_3]^+$ (100); IR (Nujol): $\tilde{\nu}=3228$ (NH stretch), 1696 (CO stretch), 1540, 1329 (NO_2 sym. and asym. stretch).

Copper(II) azacyclam complex [4](NO$_3$)$_2$: The same procedure was followed as for [**4**]$(NO_3)_2$ complex but using 4-cyanophenylurea (**9**). Yield 36%. ESI-MS (+): *m/z*: 453.2 $[M+HCOO]^+$ (100); IR (Nujol): $\tilde{\nu}=3196$ (NH stretch), 1673 (CO stretch), 2220 (CN stretching), 1327 cm^{-1} (nitrate).

X-ray crystallographic studies: Diffraction data for crystals of [**3**]$(NO_3)_2$ and [**4**]$(NO_3)_2$ were collected at ambient temperature on a conventional Enraf-Nonius CAD4 four-circle diffractometer working with graphite-monochromatised $Mo_{K\alpha}$ radiation ($\lambda=0.71073$ Å). Crystal data for the two complexes are listed in Table 2.

Data reductions (including intensity integration, background, Lorentz and polarisation corrections) were performed with the WinGX package;[43] absorption effects were evaluated with the psi-scan method,[44] and absorption correction was applied to the data (min./max. transmission factors were 0.714/0.844 and 0.834/0.902 for [**3**]$(NO_3)_2$ and [**4**]$(NO_3)_2$, respectively). Both crystal structures were solved by direct methods (SIR 97)[45] and refined by full-matrix least-square procedures on F^2 using all reflections (SHELXL 97).[46] Anisotropic displacement parameters were refined for all non-hydrogen atoms. For both molecular complexes, hy-

Table 2. Crystal data for investigated crystals.

	[**3**]$(NO_3)_2$	[**4**]$(NO_3)_2$
formula	$C_{16}H_{27}Cu\,N_9O_9$	$C_{17}H_{27}CuN_9O_7$
M	553.02	533.03
crystal dimension [mm]	$0.64\times0.45\times0.17$	$0.36\times0.29\times0.10$
crystal colour	pale red	violet
crystal system	monoclinic	monoclinic
space group	$P2_1$ (no. 4)	$P2_1/c$ (no. 14)
a [Å]	7.7883(23)	7.8787 (17)
b [Å]	10.6983(13)	14.0459(11)
c [Å]	14.0517(23)	21.5091(41)
β [°]	91.687(15)	108.294(16)
V [Å^3]	1170.3(4)	2260.0(7)
Z	2	4
ρ_{calcd} [g cm^{-3}]	1.569	1.567
$\mu(Mo_{K\alpha})$ [mm^{-1}]	1.000	1.026
scan type	ω scans	ω scans
θ range [°]	2–30	2–25
measured reflns	4415	4304
unique reflns	4003	3993
R_{int}	0.0134	0.0318
strong data [$I_O>2\sigma(I_O)$]	2925	2383
refined parameters	320	310
*R*1, *wR*2 (strong data)	0.0488, 0.0776	0.0605, 0.1223
*R*1, *wR*2 (all data)	0.1114, 0.1262	0.1381, 0.1667
GOF	1.029	1.020
max./min. residuals [e Å^{-3}]	0.88/−0.43	1.15/−0.75

drogen atoms bonded to atoms forming the penta-aza macrocyclic ring were placed at calculated positions with the appropriate AFIX instructions and refined using a riding model; the hydrogen atom bonded to the amide group of the pendant arm was located in the final ΔF maps and refined while restraining the N–H distance to be 0.90 ± 0.01 Å. The Flack parameter,[47] calculated for the non-centrosymmetric crystal of the [**3**]-$(NO_3)_2$ molecular complex, suggested that the crystal contained both enantiomers in a non-equal ratio. The refined ratio of the two components was 0.60(3):0.40(3).

CCDC-733152 and CCDC-733153 contain the supplementary crystallographic data for this paper. These data can be obtained free of charge from The Cambridge Crystallographic Data Centre via www.ccdc.cam.ac.uk/data_request/cif.

Acknowledgements

The financial support of the Italian Ministry of University and Research and of the University of Pavia is gratefully acknowledged.

[1] M. C. Thompson, D. H. Busch, *J. Am. Chem. Soc.* **1964**, *86*, 213–217.
[2] M. M. Blight, N. F. Curtis, *J. Chem. Soc.* **1962**, 3016–3020.
[3] C. D. Meyer, C. S. Joiner, J. F. Stoddart, *Chem. Soc. Rev.* **2007**, *36*, 1705–1723.
[4] a) E. K. Barefield, *Inorg. Chem.* **1972**, *11*, 2273–2274; E. K. Barefield, F. Wagner, A. W. Herlinger, A. R. Dahl, *Inorg. Synth.* **1975**, *16*, 220.
[5] E. K. Barefield, F. Wagner, K. D. Hodges, *Inorg. Chem.* **1976**, *15*, 1370–1377.
[6] I. I. Creaser, J. M. Harrowfield, A. J. Herlt, A. M. Sargeson, J. Springborg, R. J. Geue, M. R. Snow, *J. Am. Chem. Soc.* **1977**, *99*, 3181–3182.
[7] R. J. Geue, T. W. Hambley, J. M. Harrowfield, A. M. Sargeson, M. R. Snow, *J. Am. Chem. Soc.* **1984**, *106*, 5478–5488.
[8] A. M. Sargeson, *Chem. Br.* **1979**, *15*, 23–27.
[9] P. Comba, N. F. Curtis, G. A. Lawrance, A. M. Sargeson, B. W. Skelton, A. H. White *Inorg. Chem.* **1986**, *25*, 4260–4267.
[10] M. Paik Suh, S.-G. Kangl, *Inorg. Chem.* **1988**, *27*, 2544–2546.
[11] P. Comba, N. F. Curtis, G. A. Lawrance, M. A. O'Leary, B. W. Skelton, A. H. White, *J. Chem. Soc. Dalton Tram.* 1988, 2145–2152.
[12] P. V. Bernhardt, E. J. Hayes, *J. Chem. Soc. Dalton Trans.* **1998**, 3539–3541.
[13] P. Comba, Y. D. Lampeka, A. Y. Nazarenko, A. I. Prikhod'ko, H. Pritzkow, *Eur. J. Inorg. Chem.* **2002**, 1464–1474.
[14] A. De Blas, G. De Santis, L. Fabbrizzi, M. Licchelli, A. M. Manotti Lanfredi, P. Morosini, P. Pallavicini, F. Ugozzoli, *J. Chem. Soc. Dalton Trans.* **1993**, 1411–1416.
[15] F. Abbà, G. De Santis, L. Fabbrizzi, M. Licchelli, A. M. Manotti Lanfredi, P. Pallavicini, A. Poggi, F. Ugozzoli, *Inorg. Chem.* **1994**, *33*, 1366–1375.
[16] G. De Santis, L. Fabbrizzi, M. Licchelli, C. Mangano, P. Pallavicini, *Inorg. Chim. Acta* **1993**, *214*, 193–196.
[17] G. De Santis, L. Fabbrizzi, M. Licchelli, N. Sardone, A. H. Velders, *Chem. Eur. J.* **1996**, *2*, 1243–1250.
[18] L. Fabbrizzi, M. Licchelli, P. Pallavicini, *Acc. Chem. Res.* **1999**, *32*, 846–853.
[19] V. Amendola, L. Fabbrizzi, F. Foti, M. Licchelli, C. Mangano, P. Pallavicini, A. Poggi, D. Sacchi, A. Taglietti, *Coord. Chem. Rev.* **2006**, *250*, 273–299.
[20] "Amide and Urea Based Anion Receptors" P. A. Gale in *Encyclopedia of Supramolecular Chemistry*, Marcel Dekker, New York, **2004**, pp. 31–41; K. Choi, A. D. Hamilton, *J. Am. Chem. Soc.* **2003**, *125*, 10241–10249; S. O. Kang, J. M. Llinares, D. Powell, D. VanderVelde, K. Bowman-James, *J. Am. Chem. Soc.* **2003**, *125*, 10152–10153; S. Otto, S. Kubik, *J. Am. Chem. Soc.* **2003**, *125*, 7804–7805; C. R. Bondy, S. J. Loeb, *Coord. Chem. Rev.* **2003**, *240*, 77–99; S. O. Kang, M. A. Hossain, K. Bowman-James, *Coord. Chem. Rev.* **2006**, *250*, 3038–3052.
[21] B. König, M. Pelka, M. Subat, I. Dix, P. G. Jones, *Eur. J. Org. Chem.* **2001**, 1943–1949.
[22] V. J. Thöm, J. C. A. Boeyens, G. J. McDougall, R. D. Hancock, *J. Am. Chem. Soc.* **1984**, *106*, 3198–3207.
[23] K. R. Adam, I. M. Atkinson, L. F. Lindoy, *Inorg. Chem.* **1997**, *36*, 480–481.
[24] a) P. O. Whimp, M. F. Bailey, N. F. Curtis, *J. Chem. Soc. A* **1970**, 1956–1963; b) L. F. Lindoy, *The Chemistry of Macrocyclic Ligand Complexes*, Cambridge University Press, Cambridge, **1989**.
[25] a) A. De Blas, G. De Santis, L. Fabbrizzi, M. Licchelli, A. M. Manotti Lanfredi, P. Pallavicini, A. Poggi, F. Ugozzoli, *Inorg. Chem.* **1993**, *32*, 106–113; b) N. Sardone, M. Licchelli, *Acta Crystallogr. Sect. A* **1996**, *52*, 2713–2716; c) Y. D. Lampeka, S. P. Gavrish, I. M. Maloshtan, N. K. Dalley, J. D. Lamb, A. Y. Nazarenko, *Inorg. Chim. Acta* **1998**, *282*, 142–148.
[26] F. P. Schmidtchen, M. Berger, *Chem. Rev.* **1997**, *97*, 1609–1646; H-J. Schneider, A. K. Yatsimirsky *Chem. Soc. Rev.* **2008**, *37*, 263–277.
[27] Examples are provided by cage-shaped receptors containing up to six amide NH groups: K. Bowman-James, *Acc. Chem. Res.* **2005**, *38*, 671–678.
[28] M. Boiocchi, L. Del Boca, D. Esteban-Gómez, L. Fabbrizzi, M. Licchelli, E. Monzani, *J. Am. Chem. Soc.* **2004**, *126*, 16507–16514.
[29] D. Esteban-Gómez, L. Fabbrizzi, M. Licchelli, *J. Org. Chem.* **2005**, *70*, 5717–5720.
[30] M. Boiocchi, L. Del Boca, D. Esteban-Gómez, L. Fabbrizzi, M. Licchelli, E. Monzani, *Chem. Eur. J.* **2005**, *11*, 3097–3104.
[31] V. Amendola, D. Esteban-Gómez, L. Fabbrizzi, M. Licchelli, *Acc. Chem. Res.* **2006**, *39*, 343–353.
[32] P. Gans, A. Sabatini, A. Vacca, *Talanta* **1996**, *43*, 1739–1753; http://www.hyperquad.co.uk/index.htm; accessed 19 May, 2009.
[33] D. Esteban-Gómez, L. Fabbrizzi, M. Licchelli, E. Monzani, *Org. Biomol. Chem.* **2005**, *3*, 1495–1500.
[34] F. G. Bordwell, *Acc. Chem. Res.* **1988**, *21*, 456–463.
[35] B. J. Hathaway, *Struct. Bonding (Berlin)* **1984**, *57*, 55–118.
[36] A. B. P Lever, *Inorganic Electronic Spectroscopy*, Elsevier, Amsterdam, **1984**.
[37] L. Fabbrizzi, M. Licchelli, P. Pallavicini, L. Parodi, *Angew. Chem.* **1998**, *110*, 838–841; *Angew. Chem. Int. Ed.* **1998**, *37*, 800–802.
[38] P. Pallavicini, A. Perotti, A. Poggi, B. Seghi, L. Fabbrizzi, *J. Am. Chem. Soc.* **1987**, *109*, 5139–5144.
[39] J. F. J. Dippy, S. R. C. Hughes, A. Rozanski, *J. Chem. Soc.* **1959**, 2492–2498.
[40] W. D. Kumler, J. J. Eiler, *J. Am. Chem. Soc.* **1943**, *65*, 2355–2361.
[41] V. Amendola, M. Boiocchi, D. Esteban-Gómez, L. Fabbrizzi, E. Monzani, *Org . Biomol. Chem.* **2005**, *3*, 2632–2639.
[42] H. G. Hamilton, Jr., M. Alexander, *Inorg. Chem.* **1966**, *5*, 11, 2060–2061.
[43] L. J. Farrugia, *J. Appl. Crystallogr.* **1999**, *32*, 837–838.
[44] A. C. T. North, D. C. Phillips, F. S. Mathews, *Acta. Crystallogr. Sect. A* **1968**, *24*, 351–359.
[45] A. Altomare, M. C. Burla, M. Camalli, G. L. Cascarano, C. Giacovazzo, A. Guagliardi, A. G. G. Moliterni, G. Polidori, R. Spagna, *J. Appl. Crystallogr.* **1999**, *32*, 115–119.
[46] G. M. Sheldrick, SHELX97 Programs for Crystal Structure Analysis. University of Göttingen, Göttingen, Germany, **1997**.
[47] H. D. Flack, *Acta Crystallogr. Sect. A* **1983**, *39*, 876–881.

Received: May 21, 2009
Published online: September 11, 2009

